Heliyon 10 (2024) e23865

Contents lists available at ScienceDirect

Heliyon

journal homepage: www.cell.com/heliyon

An integrated strategy of UPLC-Q-TOF-MS analysis, network pharmacology, and molecular docking to explore the chemical constituents and mechanism of Zixue Powder against febrile seizures

Lingling Song [a,1], Jian Xu [a,1], Yanqiong Shi [b,1], Hemiao Zhao [a], Min Zhang [a,c], Yuefei Wang [a,c], Ying Cui [a,c,**], Xin Chai [a,c,*]

[a] National Key Laboratory of Chinese Medicine Modernization, State Key Laboratory of Component-based Chinese Medicine, Tianjin Key Laboratory of TCM Chemistry and Analysis, Tianjin University of Traditional Chinese Medicine, Tianjin, 301617, China
[b] Department of Pharmacy, Xuhui District Central Hospital, Shanghai, 200031, China
[c] Haihe Laboratory of Modern Chinese Medicine, Tianjin, 301617, China

ARTICLE INFO

Keywords:
Zixue powder
Febrile seizures
UPLC-Q-TOF-MS
Network pharmacology
Molecular docking

ABSTRACT

Febrile seizures (FS) are the most common type of seizures for children. As a commonly used representative cold formula for resuscitation, Zixue Powder (ZP) has shown great efficacy for the treatment of FS in clinic, while its active ingredients and underlying mechanism remain largely unclear. This study aimed to preliminarily elucidate the material basis of ZP and the potential mechanism for the treatment of FS through ultra-performance liquid chromatography coupled with quadrupole time-of-flight mass spectrometry (UPLC-Q-TOF-MS), network pharmacology, and molecular docking. UPLC-Q-TOF-MS was firstly applied to characterize the ingredients in ZP, followed by network pharmacology to explore the potential bioactive ingredients and pathways of ZP against FS. Furthermore, molecular docking technique was employed to verify the binding affinity between the screened active ingredients and targets. As a result, 75 ingredients were identified, containing flavonoids, chromogenic ketones, triterpenes and their saponins, organic acids, etc. Through the current study, we focused on 13 potential active ingredients and 14 key potential anti-FS targets of ZP, such as IL6, STAT3, TNF, and MMP9. Gene Ontology and Kyoto Encyclopedia of Genes and Genomes enrichment analysis showed that inflammatory response, EGFR tyrosine kinase inhibitor resistance, AGE-RAGE signaling pathway in diabetic complications, and neuroactive ligand-receptor interaction were the main anti-FS signaling pathways.

Abbreviations: BP, biological process; CC, cellular component; CX, Chenxiang; DX, Dingxiang; FS, febrile seizures; GC, Gancao; GO, Gene Ontology; KEGG, Kyoto Encyclopedia of Genes and Genomes; MCC, maximal clique centrality; MF, molecular function; MW, molecular weight; MX, Muxiang; PPI, Protein-Protein Interaction; SM, Shengma; TCM, traditional Chinese medicine; TCMSP, Traditional Chinese Medicine Systems Pharmacology Database and Analysis Platform; TIC, total ion chromatogram; UPLC-Q-TOF-MS, ultra-performance liquid chromatography coupled with quadrupole time-of-flight mass spectrometry; XS, Xuanshen; ZP, Zixue Powder.

* Corresponding author. National Key Laboratory of Chinese Medicine Modernization, State Key Laboratory of Component-based Chinese Medicine, Tianjin Key Laboratory of TCM Chemistry and Analysis, Tianjin University of Traditional Chinese Medicine, Tianjin 301617, China
** Corresponding author. National Key Laboratory of Chinese Medicine Modernization, State Key Laboratory of Component-based Chinese Medicine, Tianjin Key Laboratory of TCM Chemistry and Analysis, Tianjin University of Traditional Chinese Medicine, Tianjin, 301617, China.
E-mail addresses: CQL8179270@tjutcm.edu.cn (Y. Cui), chaix0622@tjutcm.edu.cn (X. Chai).
[1] These authors contributed equally to this work.

https://doi.org/10.1016/j.heliyon.2023.e23865
Received 21 August 2023; Received in revised form 14 December 2023; Accepted 14 December 2023
Available online 15 December 2023

Licochalcones A and B, 26-deoxycimicifugoside, and hederagenin were screened as the main potential active ingredients by molecular docking. In conclusion, this study provides an effective in-depth investigation of the chemical composition, potential bioactive components, and possible anti-FS mechanism of ZP, which lays the foundation for pharmacodynamic studies and clinical applications of ZP.

1. Introduction

Febrile seizures (FS) are the most common convulsive disease for infants and children aged 6 months to 5 years, affecting 2–5% of children worldwide [1–3]. Studies have shown that recurrent FS may increase the risk of temporal lobe epilepsy, psychiatric disease, and even death [4,5]. The occurrence of FS has been linked to inflammation, familial history, and deficiencies of certain elements (iron, selenium, and zinc) [6–9]. In clinical practice, anticonvulsant drugs, such as phenobarbital, diazepam, and valproic acid, have been used to treat FS [10]. According to traditional Chinese medicine (TCM) theory, FS belong to the category of "acute convulsion", and the curing principle for FS is to relieve spasm, clear heat, eliminate phlegm, relieve shock, and calm wind [11], which has been proved to be effective for FS [12].

Zixue Powder (ZP) is a classical Chinese herbal formula for FS in children, composed of 16 TCMs, including Gypsum Fibrosum (Shigao), Gypsum Rubrum (Beihanshuishi), Talcum (Huashi), Magnetitum (Cishi), Scrophulariae Radix (Xuanshen, XS), Cimicifugae Rhizoma (Shengma, SM), Glycyrrhizae Radix et Rhizoma (Gancao, GC), Caryophylli Flos (Dingxiang, DX), Aucklandiae Radix (Muxiang, MX), Aquilariae Lignum Resinatum (Chenxiang, CX), Natrii Sulfas (Mangxiao), Nitre (Xiaoshi), Powerdered Buffalo Horn Extract (Shuiniujiaonongsuofen), Saigae Tataricae Cornu (Lingyangjiaofen), artificial Mosk (Rengongshexiang), and Cinnabaris (Zhusha) [13]. ZP can clear heat and induce resuscitation, relieve spasmolysis and tranquilize based on TCM theory. Modern pharmacological studies have demonstrated that ZP has antipyretic, sedative, anti-inflammatory, and anticonvulsant effects [14,15]. At present, ZP has been frequently used in the clinical treatment of children with FS, septic shock, etc [16]. However, no comprehensive studies have been conducted to explore the chemical constituents in ZP and the underlying mechanisms for anti-FS.

Network pharmacology is an integrated approach that blends the disciplines of systems biology and bioinformatics and network science to investigate the underlying molecular mechanisms between drugs and therapeutic targets, which has been frequently used in the research of TCM [17]. Meanwhile, molecular docking can be used to screen active ingredients by predicting the binding affinity between ingredients and proteins, which is a method widely used in drug discovery [18,19]. The combination of network pharmacology and molecular docking allows for greater efficiency on screening active ingredients and identifying their potential targets in TCM [20].

In this research, we identified the possible active compounds and the potential molecular action mechanisms of ZP against FS. A fast and effective method was developed for the chemical characterization of ZP based on ultra-performance liquid chromatography coupled with quadrupole time-of-flight mass spectrometry (UPLC-Q-TOF-MS), and a strategy combined with network pharmacology and molecular docking was further used to explore the underlying action mechanism of ZP against FS. This study provides a reference for clinical practice and further research on ZP.

2. Materials and methods

2.1. Materials and reagents

Reference standards including agarotetrol, isoferulic acid, and harpagide were obtained from National Institutes for Food and Drug Control (Beijing, China). Liquiritigenin, isoliquiritigenin, angoroside C, cimicifugine, glycyrrhizic acid, liquiritin, liquiritin apioside, isoliquiritin, *trans*-cinnamic acid, harpagoside, sucrose, formononetin, and licochalcone A were purchased from Shanghai Yuanye Bio-Technology Co., Ltd. (Shanghai, China). The purities of all the reference substances were higher than 98 %.

ZP samples were provided by Tianjin Hongrentang Pharmaceutical Co., Ltd. (Tianjin, China). LC-MS grade methanol was purchased from Sigma-Aldrich (St. Louis, MO, USA). Formic acid was purchased from Shanghai Aladdin Biochemical Technology Co., Ltd. (Shanghai, China). Water used for UPLC-Q-TOF-MS analysis was purified by Milli-Q water purification system (Millipore, Billerica, MA, USA).

2.2. Preparation of reference and sample solutions

Sixteen reference compounds were accurately weighed and respectively dissolved in methanol as stock solutions except for sucrose dissolved in water. An appropriate amount of each reference stock solution was accurately transferred in a 10 mL volumetric flask and diluted with 75 % aqueous methanol (*v/v*) to obtain the mixed solution at the concentrations of 0.0521 mg/mL harpagide, 0.0500 mg/mL liquiritin, 0.0501 mg/mL cimicifugin, 0.0555 mg/mL isoliquiritin, 0.0501 mg/mL agarotetrol, 0.0581 mg/mL apioside liquiritin, 0.0500 mg/mL angoroside C, 0.0503 mg/mL liquiritigenin, 0.0500 mg/mL isoferulic acid, 0.0501 mg/mL isoliquiritigenin, 0.0502 mg/mL harpagoside, 0.0511 mg/mL glycyrrhizic acid, 0.0500 mg/mL *trans*-cinnamic acid, 0.0304 mg/mL licoricechalcone A, 0.0487 mg/mL sucrose, and 0.0560 mg/mL formononetin.

1.0 g of ZP was accurately weighed and transferred into a conical flask and ultrasonically extracted at 60 °C by 75 % aqueous

methanol for 30 min, then cooled to ambient temperature and diluted to scale by adding 75 % aqueous methanol. The extracted solution was centrifuged at 12700 rpm for 10 min to obtain the supernatant. All the standard and sample solutions were stored at 4 °C when not in use.

2.3. UPLC-Q-TOF-MS analysis

Chemical analysis was conducted on an Acquity UPLC I Class system (Waters Corporation, Milford, MA, USA) equipped with XEVO G2-XS quadrupole time-of-flight mass spectrometry (Waters Corp.). UPLC analysis was performed on the Agilent ZORBAX SB-C18 column (4.6 × 100 mm, 1.8 μm, Agilent, Santa Clara, CA, USA) using a flow rate of 0.5 mL/min at 45 °C for chromatographic separation. The mobile phase consisted of methanol (A) and 0.1 % formic acid (B), using a gradient elution of 10–52 % A for 0–8 min, 52–58 % A for 8–12 min, and 58–95 % A for 12–20 min. The injection volume was 2 μL.

The mass spectrometric detection was operated on Waters Xevo G2-XS QTOF mass spectrometer equipped with ESI source in both positive and negative modes from *m/z* 100–1500 Da. Detailed mass spectrometric parameters were set as follows: the capillary voltage was set at 3.00 kV (ESI^+) and −2.5 kV (ESI^-); the ion source temperature was 120 °C; the sample cone voltage was 40 V; the cone gas flow was set at 50 L/h; the desolvation temperature was set at 500 °C; the desolvation gas flow was 800 L/h. The low collision energy was 6 eV and the high collision energy was 10∼45 eV.

2.4. Network pharmacology analysis

2.4.1. Target genes of the identified compounds related to FS

The structures of compounds in ZP were downloaded from PubChem (https://pubchem.ncbi.nlm.nih.gov/) and saved in SDF format, which were submitted to SwissTargetPrediction database (http://www.swisstargetprediction.ch/) and Traditional Chinese Medicine Systems Pharmacology Database and Analysis Platform (TCMSP, https://www.tcmsp-e.com/) for the targets prediction of the focused compounds with the species "*Homo sapiens*". All the proteins obtained previously were converted to the official symbol formats for genes using UniProt database (https://www.uniprot.org/). Meanwhile, the FS-related targets were obtained from GeneCards database (https://www.genecards.org/) and Online Mendelian Inheritance in Man database (OMIM, https://www.omim.org/). Then, the common targets between the predicted targets of chemical compounds and FS were obtained by Venny 2.1 platform (https://bioinfogp.cnb.csic.es/tools/venny/index.html), which were considered as potential therapeutic targets. To further illustrate the mechanism, Cytoscape 3.9.1 software was used for the visualization of the interactions among TCMs, ingredients, and targets in ZP. The potential bioactive compounds were screened according to the degree values, which were used as key parameters to reflect the importance of nodes.

2.4.2. Gene Ontology (GO) and Kyoto Encyclopedia of genes and genomes (KEGG) pathway enrichment analysis

The common genes were imported into DAVID database (https://david.ncifcrf.gov/) to perform GO and KEGG pathway enrichment analysis with species restricted to "*Homo sapiens*". The results of biological process (BP), cellular component (CC), and molecular function (MF) of GO enrichment analysis, and KEGG pathway analysis were downloaded and saved as TXT, respectively. Go terms and KEGG pathways were visualized by Bioinformatics (http://www.bioinformatics.com.cn/) with *P*-value <0.05.

2.4.3. Construction of protein-protein interaction (PPI) network

Targets of the common genes were imported into STRING (https://cn.string-db.org/) database. The species was limited to "*Homo sapiens*" in the operation interface, and the confidence score was set up to 0.70 (higher confidence). Cytoscape 3.9.1 software was used to construct the PPI network, and the core targets were screened by two algorithms of maximal clique centrality (MCC) and degree value, which could improve accuracy of the results.

Table 1
Detailed information on the crystal structures of the targets.

No.	Full name of the protein	Abbreviation	PDB ID	Resolution (Å)	References
1	Serine/threonine kinase 1	AKT1	3O96, 6HHF	2.70, 2.90	[21,22]
2	Epidermal growth factor receptor	EGFR	2GS6	2.60	[23]
3	Fibroblast growth factor 2	FGF2	5X1O	1.90	[24]
4	Ierleukin-1β	IL1B	5R88	1.48	[25]
5	Ierleukin-2	IL2	1M49	2.00	[26]
6	Matrix metalloproteinase-9	MMP9	2OVZ, 4XCT	2.00, 1.30	[27,28]
7	Protein tyrosine phosphatase non-receptor type 11	PTPN11	3MOW	2.30	[29]
8	Signal transducer and activator of transcription 3	STAT3	5AX3, 6NUQ	2.98, 3.15	[30,31]
9	Toll-like receptor 4	TLR4	4G8A	2.40	[32]
10	Tumor necrosis factor	TNF	2AZ5	2.10	[33]
11	Tumor protein 53	TP53	4BV2	3.30	[34]

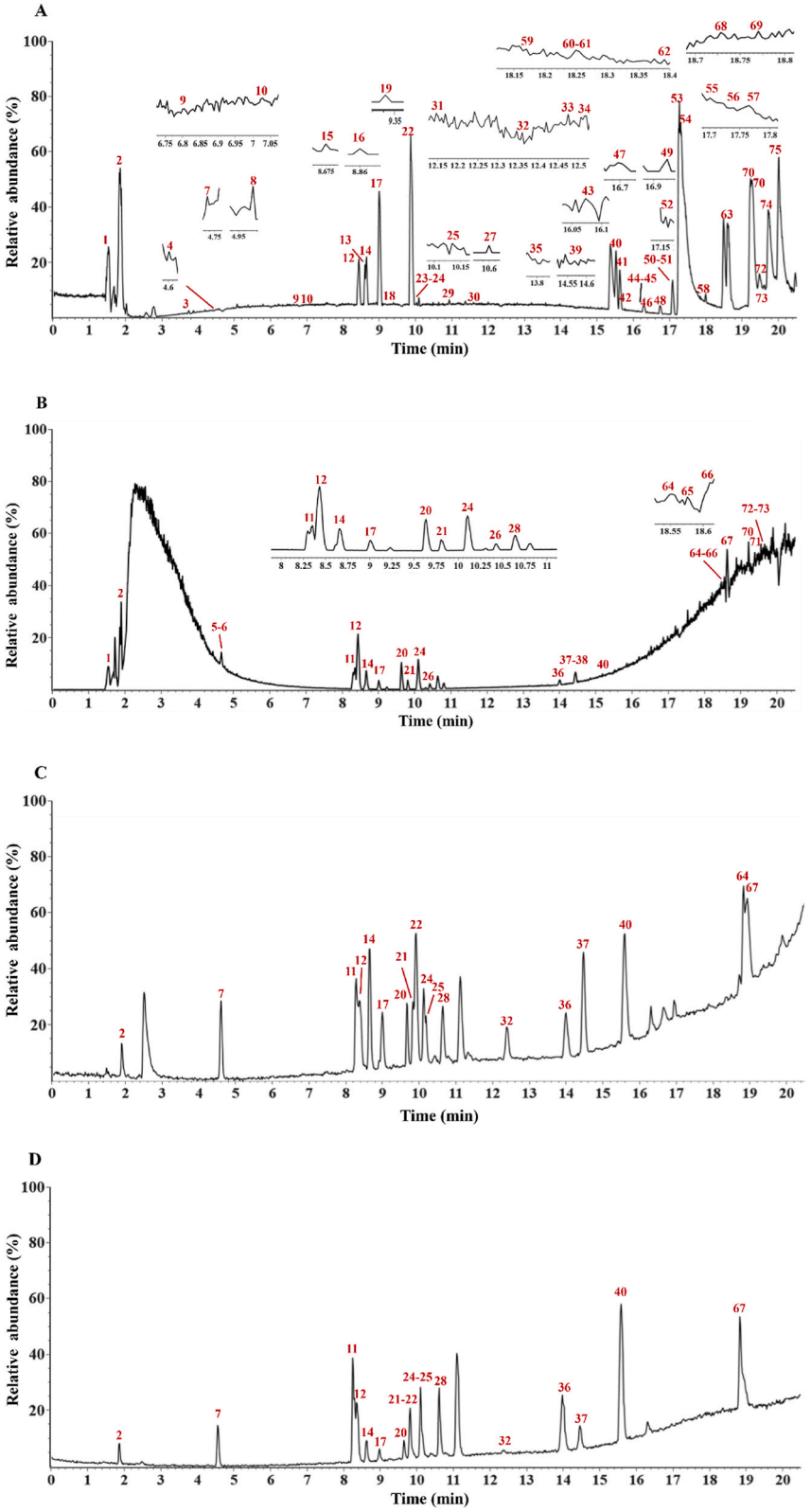

Fig. 1. Total ion chromatograms of ZP in the positive (A) and negative ion modes (B) and reference compounds in the positive (C) and negative ion modes (D).

Table 2
Information of the identified compounds from Zixue Powder by UPLC-Q-TOF-MS.

No.	Compounds	Formula	t_R (min)	Quasi-molecular ion/adduct ion	Measured mass (MW)	Calculated mass (MW)	Error (ppm)	Fragment ions (*m/z*)	Source
1	Mokko lactone	$C_{15}H_{20}O_2$	1.54	$[M+H]^+$	232.1459	232.1463	−1.7	189.0972, 161.0955	MX
2*	*D*-(+)-sucrose	$C_{12}H_{22}O_{11}$	1.86	$[M+Na]^+$	342.1156	342.1162	−1.7	277.0887, 203.0519, 185.0409	XS
3	Fukiic acid	$C_{11}H_{12}O_8$	3.74	$[M+Na]^+$	272.0522	272.0532	−3.6	209.0433, 191.0329, 163.0381, 135.0424	SM
4	Cimidahurinie	$C_{14}H_{20}O_8$	4.61	$[M+Na]^+$	316.1153	316.1158	−1.6	177.0534, 127.0314	SM
5	Piscidic acid	$C_{11}H_{12}O_7$	4.67	$[M-H]^-$	256.0572	256.0580	−4.1	183.0668, 147.0428, 119.0478, 91.0526	SM
6	Ningpogenin	$C_9H_{14}O_3$	4.68	$[M-H]^-$	170.0931	170.0943	−5.9	107.0477, 91.0526, 77.0368	XS
7*	Harpagide	$C_{15}H_{24}O_{10}$	4.73	$[M+Na]^+$	364.1358	364.1370	−3.0	279.0926, 167.0695, 135.0429, 123.0426	XS
8	4-Methoxycinnamic acid	$C_{10}H_{10}O_3$	4.97	$[M+NH_4]^+$	178.0621	178.0630	−4.8	165.0545, 119.0475	XS
9	Verbascoside	$C_{29}H_{36}O_{15}$	6.80	$[M+Na]^+$	624.2063	624.2054	1.4	569.1922, 485.1601, 279.0928, 201.0454	XS
10	Shomaside B	$C_{27}H_{30}O_{15}$	7.04	$[M+H]^+$	594.1564	594.1585	−3.6	577.1509, 457.1156, 273.0752, 163.0377	SM
11*	Liquiritin apioside	$C_{26}H_{30}O_{13}$	8.33	$[M+Na]^+$	550.1681	550.1686	−0.9	413.1201, 163.0381	GC
12*	Liquiritin	$C_{21}H_{22}O_9$	8.43	$[M+Na]^+$	418.1261	418.1264	−0.7	257.0808, 239.0697, 163.0379, 137.0224	GC
13	Prim-*O*-glucosylcimifugin	$C_{22}H_{28}O_{11}$	8.60	$[M+H]^+$	468.1628	468.1632	−0.7	451.1621, 409.1106, 307.1171	SM
14*	Agarotetrol	$C_{17}H_{18}O_6$	8.64	$[M+H]^+$	318.1100	318.1103	−0.3	301.0944, 283.0865, 255.0901, 227.5403	CX
15	Cimicifugamide	$C_{25}H_{31}NO_{10}$	8.67	$[M+H]^+$	505.1946	505.1948	−0.4	407.0903, 255.1011	SM
16	Sophoraflavone B	$C_{21}H_{20}O_9$	8.86	$[M+H]^+$	416.1097	416.1107	−2.5	255.0645, 133.0839, 89.0578	GC
17*	Isoferulic acid	$C_{10}H_{10}O_4$	9.00	$[M+H]^+$	194.0571	194.0579	−3.9	177.0539, 149.0589, 134.0351, 105.0317	XS
18	Sibirioside A	$C_{21}H_{28}O_{12}$	9.14	$[M+Na]^+$	472.1559	472.1581	−4.4	333.0943, 273.0753, 131.0481	XS
19	Isoliquiritin apioside	$C_{26}H_{30}O_{13}$	9.31	$[M+H]^+$	550.1684	550.1686	−0.2	429.2017, 417.1950, 255.1152, 135.0328	GC
20*	Angoroside C	$C_{36}H_{48}O_{19}$	9.62	$[M+Na]^+$	784.2805	784.2790	1.9	507.1853, 339.1065, 177.0539	XS
21*	Neoisoliquritin	$C_{26}H_{30}O_{13}$	9.81	$[M+H]^+$	550.1684	550.1686	−0.4	419.1330, 257.0802, 147.0434	GC

(*continued on next page*)

Table 2 (*continued*)

No.	Compounds	Formula	t_R (min)	Quasi-molecular ion/adduct ion	Measured mass (MW)	Calculated mass (MW)	Error (ppm)	Fragment ions (*m/z*)	Source
22*	Cimicifugin	$C_{16}H_{18}O_6$	9.88	$[M+H]^+$	306.1099	306.1103	−1.3	273.0752, 259.0595, 235.0594	SM
23	8-*O*-Feruloylharpagide	$C_{25}H_{32}O_{13}$	10.07	$[M+Na]^+$	540.1863	540.1843	3.6	419.1330, 285.0737, 249.0372, 137.0221	XS
24	Neoliquiritin isomer	$C_{21}H_{22}O_9$	10.11	$[M+H]^+$	418.1260	418.1264	−0.9	257.0805, 239.0691, 177.0535, 137.0222	GC
25*	Angoroside C isomer	$C_{36}H_{48}O_{19}$	10.13	$[M+Na]^+$	784.2792	784.2790	0.3	661.2090, 419.1330, 339.1094, 177.0535	XS
26	Ononin	$C_{22}H_{22}O_9$	10.41	$[M-H]^-$	430.1263	430.1264	−0.1	291.0618, 269.0806, 97.0268	GC
27	Licochalcone B	$C_{16}H_{14}O_5$	10.61	$[M+H]^+$	286.0836	286.0841	−1.8	257.0805, 163.0384, 137.0222, 111.0425	GC
28*	Liquiritigenin	$C_{15}H_{12}O_4$	10.64	$[M-H]^-$	256.0733	256.0736	−1.0	163.0384, 137.0222, 119.0477	GC
29	Cimicifugic acid E	$C_{21}H_{20}O_{10}$	11.08	$[M+Na]^+$	432.1046	432.1057	−2.3	283.0860, 177.0534, 137.0585	SM
30	Norcimifugin	$C_{15}H_{16}O_6$	11.72	$[M+H]^+$	292.0941	292.0947	−2.0	257.0800, 233.0447, 137.0587	SM
31	Daidzein	$C_{15}H_{10}O_4$	12.15	$[M+H]^+$	254.0574	254.0579	−2.1	149.0585, 137.0212, 121.0296	GC
32*	*trans*-Cinnamic acid	$C_9H_8O_2$	12.36	$[M+H]^+$	148.0523	148.0524	−0.8	131.0479, 103.0524, 77.0365	XS
33	Medicarpin	$C_{16}H_{14}O_4$	12.49	$[M+H]^+$	270.0882	270.0892	−3.6	229.0845, 163.0741, 107.0483	GC
34	(23*R*,24*S*)-25-*O*-acetyl-ciminol-3-*O*-*β*-D-xylopyranoside	$C_{37}H_{58}O_{10}$	12.50	$[M+Na]^+$	662.4034	662.4030	8.7	535.2902, 527.2986, 185.1321	SM
35	Alantolactone	$C_{15}H_{20}O_2$	13.81	$[M+H]^+$	232.1458	232.1463	−2.4	187.1474, 161.0592, 149.0979	MX
36*	Isoliquiritigenin	$C_{15}H_{12}O_4$	14.02	$[M+H]^+$	256.0733	256.0736	−1.1	239.0695, 163.0374, 137.0220, 119.0477	GC
37*	Harpagoside	$C_{24}H_{30}O_{11}$	14.42	$[M+Na]^+$	494.1788	494.1788	−0.1	369.1153, 327.1224, 149.0588	XS
38	6-Methoxy-2-[2- (3′-methoxy-4′-hydroxyphenyl) ethyl] chromone	$C_{19}H_{18}O_5$	14.44	$[M+H]^+$	326.1151	326.1154	−1.1	187.0782, 149.0588, 121.0632	CX
39	2′-*O*-Acetyl-cimicifugoside H-1	$C_{37}H_{54}O_{10}$	14.57	$[M+H]^+$	658.3695	658.3717	−3.3	521.2921, 469.3361, 261.1303	SM
40*	Formononetin	$C_{16}H_{12}O_4$	15.50	$[M+H]^+$	268.0732	268.0736	−1.4	253.0500, 237.0542, 107.0473	GC
41	Cimicifugoside H2	$C_{35}H_{54}O_{10}$	15.64	$[M+H]^+$	634.3714	634.3717	−0.4	481.2959, 469.3310, 161.0954	SM
42	Isoalantolactone	$C_{15}H_{20}O_2$	15.74	$[M+H]^+$	232.1450	232.1463	−5.7	205.1569, 187.0458, 91.0530	MX

(*continued on next page*)

Table 2 (*continued*)

No.	Compounds	Formula	t_R (min)	Quasi-molecular ion/adduct ion	Measured mass (MW)	Calculated mass (MW)	Error (ppm)	Fragment ions (*m/z*)	Source
43	Glabrolide	$C_{30}H_{44}O_4$	18.26	$[M+H]^+$	468.3235	468.3240	−1.0	451.3193, 317.2129, 271.2055, 235.1659	GC
44	26-Deoxycimicifugoside	$C_{37}H_{54}O_{10}$	16.30	$[M+H]^+$	658.3691	658.3717	−4.0	451.3199, 379.2615, 335.2384, 171.1164	SM
45	7β-Hydroxy-cimigenol xyloside	$C_{35}H_{56}O_{10}$	16.33	$[M+Na]^+$	636.3877	636.3874	0.5	339.1992, 311.1679, 297.1521	SM
46	Cimigemol	$C_{30}H_{48}O_5$	16.41	$[M+Na]^+$	488.3521	488.3502	3.8	453.3345, 315.1972, 189.1628, 159.1168	SM
47	Cimiside A	$C_{35}H_{56}O_{10}$	16.70	$[M+H]^+$	636.3870	636.3874	−0.5	619.3841, 511.3408, 451.3189, 315.1589	SM
48	Hederagenin	$C_{30}H_{48}O_4$	16.79	$[M+Na]^+$	472.3573	472.3553	4.1	337.2548, 241.1969, 233.1541, 149.1311	CX
49	6-Hydroxy-2-[2-(4′-methoxyphenyl) ethyl] chromone	$C_{18}H_{16}O_4$	16.93	$[M+H]^+$	296.1041	296.1049	−2.5	121.0639	CX
50	(3β,12β,16β)-12-Acetoxy-16,23-epoxy-9,19-cyclolanolin-22- en-24-one-3-*O*-β-D-pyranoside	$C_{37}H_{56}O_9$	17.10	$[M+Na]^+$	644.3869	644.3924	−8.1	547.3284, 495.3454, 313.1796	SM
51	(−)-Bornyl ferulate	$C_{20}H_{26}O_4$	17.10	$[M+Na]^+$	330.1823	330.1831	−2.3	313.1795, 293.1736, 105.0685	CX
52	6-Hydroxy-2- (2-phenylethyl) chromone	$C_{17}H_{14}O_3$	17.17	$[M+H]^+$	266.0940	266.0943	−1.0	177.0522, 147.0455, 91.0528	CX
53	Cimidahuside J	$C_{37}H_{56}O_{11}$	17.24	$[M–H+HCOOH]^-$	676.3784	676.3823	−5.4	645.3246, 339.1992, 311.1678, 297.1521	SM
54	Baimuxinfuranic acid	$C_{15}H_{24}O_3$	17.32	$[M+Na]^+$	252.1743	252.1725	6.4	189.1652, 175.1108, 121.0999	CX
55	12β-Hydroxycimigenol	$C_{30}H_{48}O_6$	17.72	$[M+Na]^+$	504.3443	504.3451	−1.4	453.3365, 371.2265, 259.2075, 123.0787	SM
56	Licobenzofuran	$C_{21}H_{22}O_5$	17.75	$[M+H]^+$	354.1450	354.1467	−4.9	341.1392, 299.0885, 121.0639	GC
57	6,7-Dimethoxy-2-[2-(*p*-methoxyphenyl) ethyl] chromone	$C_{20}H_{20}O_5$	17.78	$[M+H]^+$	340.1302	340.1311	−2.5	299.0885, 181.0476, 121.0639	CX
58	6,7-Dimethoxy-2-phenethylchromone	$C_{19}H_{18}O_4$	18.00	$[M+H]^+$	310.1203	310.1205	−0.6	205.0486, 181.0484, 91.0531	CX
59	7α,15-Dihydroxydehydroabietic acid	$C_{20}H_{28}O_4$	18.18	$[M+H]^+$	332.1984	332.1988	−1.2	315.1945, 251.1813, 201.1290, 161.1310	CX
60	Isoglabrolide	$C_{30}H_{44}O_4$	18.26	$[M+H]^+$	468.3235	468.3240	−1.0	451.3193, 317.2129, 271.2055, 235.1659	GC
61	Uralsaponin N	$C_{42}H_{62}O_{17}$	18.26	$[M+H]^+$	838.4001	838.3987	1.7	645.3631, 469.3304, 451.3193, 297.1841	GC

(*continued on next page*)

Table 2 (*continued*)

No.	Compounds	Formula	t_R (min)	Quasi-molecular ion/adduct ion	Measured mass (MW)	Calculated mass (MW)	Error (ppm)	Fragment ions (*m/z*)	Source
62	Cimifoetiside V	$C_{47}H_{76}O_{19}$	18.38	$[M–H+HCOOH]^-$	944.4986	944.4981	0.5	793.4013, 711.3939, 483.3102, 185.0093	SM
63	AH14	$C_{34}H_{30}O_8$	18.53	$[M+H]^+$	566.1928	566.1941	−2.2	383.1503, 337.1065, 145.0626	CX
64*	Licochalcone A	$C_{21}H_{22}O_4$	18.56	$[M+H]^+$	338.1514	338.1518	−1.1	323.1304 237.0588, 205.1206, 121.0268	GC
65	Licoricone	$C_{22}H_{22}O_6$	18.57	$[M+H]^+$	382.1413	382.1416	−0.9	327.0855, 283.0586, 191.0703, 137.0224	GC
66	2-(2-Phenylethyl) chromone	$C_{17}H_{14}O_2$	18.62	$[M+H]^+$	250.0992	250.0994	−0.6	133.1007, 107.0844, 91.0527	CX
67*	Glycyrrhizinic acid	$C_{42}H_{62}O_{16}$	18.62	$[M−H]^-$	822.4054	822.4038	2.0	759.3958, 645.3623, 351.0560, 193.0342	GC
68	24-*O*-Acetyl-7,8 - dihydro-lignoside	$C_{37}H_{58}O_{11}$	18.72	$[M+Na]^+$	678.3976	678.3979	−0.5	565.3153, 451.3191, 393.2807, 195.1205	SM
69	Cimidahuside I	$C_{37}H_{58}O_{11}$	18.76	$[M–H+HCOOH]^-$	678.3982	678.3979	0.4	645.3265, 339.1994, 311.1681, 297.1525	SM
70	6-Methoxy-2-(2-phenylethyl) chromone	$C_{18}H_{16}O_3$	19.26	$[M+H]^+$	280.1099	280.1099	−0.2	131.0841, 57.0696	CX
71	Cimicifoetiside A	$C_{37}H_{58}O_{10}$	19.35	$[M+Na]^+$	662.4034	662.4030	0.6	609.3958, 565.3703, 229.1406	SM
72	Cimifoetiside IV isomer	$C_{43}H_{68}O_{15}$	19.50	$[M+Na]^+$	824.4574	824.4558	1.9	807.4518, 645.3987, 453.3349, 221.1374	SM
73	Cimiside D	$C_{43}H_{70}O_{16}$	19.67	$[M+Na]^+$	842.4681	842.4664	2.0	283.2030, 163.1113	SM
74	Isocostic acid	$C_{15}H_{22}O_2$	19.73	$[M+H]^+$	234.1614	234.1620	−2.3	163.0753 107.0838, 77.0371	MX
75	Cimifoetiside IV	$C_{43}H_{68}O_{15}$	19.94	$[M+Na]^+$	824.4581	824.4558	2.7	761.4809, 665.4278, 221.1371, 117.0899	SM

Notes: MW: Molecular Weight; MX: Muxiang; XS: Xuanshen; SM: Shengma; GC: Gancao; CX: Chenxiang, *: compared with reference standards.

2.5. Molecular docking verification

The crystal structures of the targets were acquired from the RCSB Protein Data Bank (https://www.rcsb.org/), whose detailed information was displayed in Table 1. The tested compound's structure files (mol2 format) were downloaded from TCMSP database, and then converted into a 3D structure using Chem 3D 19.0. Then, the 3D structures of target proteins and compounds were imported into Discovery Studio 2020 software. The test compounds as ligands were prepared to constrain the optimal conformation. The target proteins were prepared by removing water molecules, adding hydrogen, fixing the missing residues or rings, and defining the active center. The tested compound was then docked to the target by CDocker module, from which the CDocker interaction energy scores were ranked to predict the interaction capacity. Based on the CDocker interaction energy value, the interaction between the ligand and the receptor was quantified, with the lower energy indicating the stronger interaction.

2.6. Data processing

The information of chemical compounds from ZP was collected, which was combined with the UNIFI Chinese medicine database to establish the chemical constituents database of ZP. The MS data were collected in MS^E mode and analyzed by MassLynx 4.1 software

and the UNIFI database (Waters Corp.). The compounds were characterized based on the fragments matching with errors less than 10 ppm. Furthermore, the standards and related literatures were used to check the accuracy and reliability of identified results. The common targets between the predicted targets of chemical compounds and FS were visualized by Venny 2.1 platform. The visual analysis of network pharmacology was completed by Cytoscape 3.9.1 software. The docked complexes were visualized and converted in PDB files for 2D-3D interactive visualization study with the help of PyMol 2.4.1 software.

3. Results and discussion

3.1. Chemical profiling of ZP by UPLC-Q-TOF-MS

A method for the separation and identification of the chemical constituents of ZP was established based on UPLC-Q-TOF-MS technology. The total ion chromatograms of ZP and related standards in the positive and negative ion modes were presented in Fig. 1A–D. A total of 75 compounds in ZP were identified, including 19 triterpenoids and their glycosides, 17 flavonoids, 13 chromones, six organic acids, six sesquiterpenes, five phenylpropanoids, four monoterpenes, and five other compounds.

Among them, 16 compounds (compounds 2, 7, 11, 12, 14, 17, 20, 21, 22, 28, 32, 36, 37, 40, 64, and 67) were confirmed by comparing the retention times and mass fragments with that of authentic standards. While other compounds were preliminarily characterized based on their highly accurate quasi-molecular ions/adduct ions such as $[M+H]^+$, $[M-H]^-$, $[M-H+HCOOH]^-$, and $[M+Na]^+$ as well as mass fragmentation recorded in the self-built ZP UNIFI database. For 75 compounds, the detailed informations including retention time (t_R), molecular formula, nomenclature, calculation and determination of molecular weight, fragment ions, and source were provided in Table 2.

3.2. Network analysis for FS-related targets of ZP

ZP is a representative cold formula for resuscitation, which is known as the three most effective formulas for warm disease together with Angong Niuhuang pill and Zhibao Dan. It shows favorable clinical effects on FS in children [35], which also has been demonstrated to exert therapeutic effects on collagen-induced arthritis injury in rats through anti-inflammatory and antioxidant effects [15]. Additionally, ZP can play an anticonvulsive role by reducing the content of the excitatory neurotransmitter glutamate in the cerebral cortex of convulsive mice [36].

In this study, 786 protein targets from 75 compounds in ZP were obtained from the SwissTargetPrediction and TCMSP databases. The targets of each compound were provided in Table S1. Through the Genecards and OMIM databases, 2194 FS-associated targets were obtained, and the pertinent data were shown in Table S2. As shown in Venn diagram, 206 common genes were identified as candidate targets of ZP in the treatment of FS. In order to further screen the active compounds in ZP, the "TCMs-compounds-targets" network was constructed (Fig. 2). Cytoscape plug-in was used to perform topological analysis, and active compounds were screened according to degree >20. As a result, ZP might exhibit therapeutic effects on FS through 21 potential bioactive compounds, such as 2-(2-phenylethyl) chromone, isoliquiritin, 6-hydroxy-2-(2-phenylethyl) chromone, licochalcone A, liquiritigenin, cimicifugine, and so on. More details were included in Table S3. These compounds may be the key active compounds in ZP for treating FS. Besides, the results also revealed that different compounds from ZP might exert a therapeutic effect by targeting the same genes.

3.3. GO and KEGG pathway enrichment analysis

GO terms (BP, CC, and MF) and KEGG pathways were enriched from the 206 common targets ($P < 0.05$) via DAVID database. The top ten terms for BP, CC, and MF were respectively visualized in Fig. 3A. The main enrichment items of BP included cytokines mediation, inflammatory response, positive regulation of MAPK cascade pathway, hypoxia response, positive regulation of MAP kinase

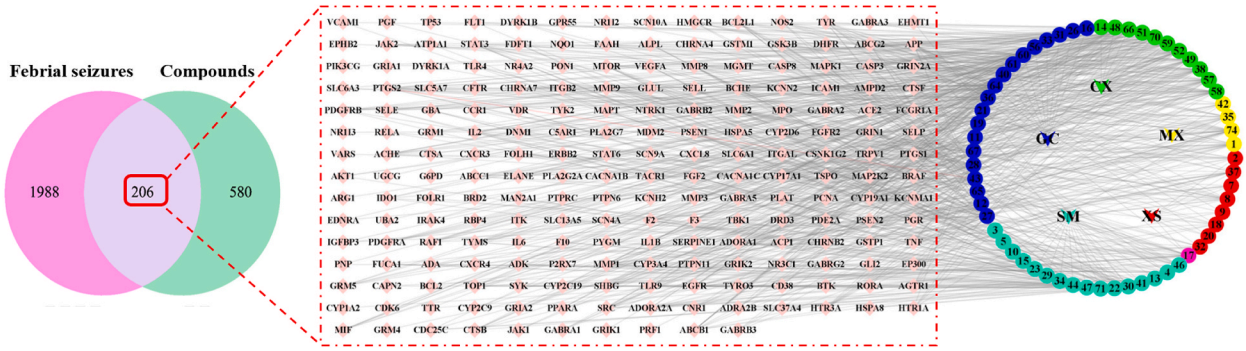

Fig. 2. "TCMs-compounds-targets" network. (The V-shaped, circular, and pink diamond-shaped nodes represent TCMs, chemical compounds, and 206 potential targets, respectively.). (For interpretation of the references to color in this figure legend, the reader is referred to the Web version of this article.)

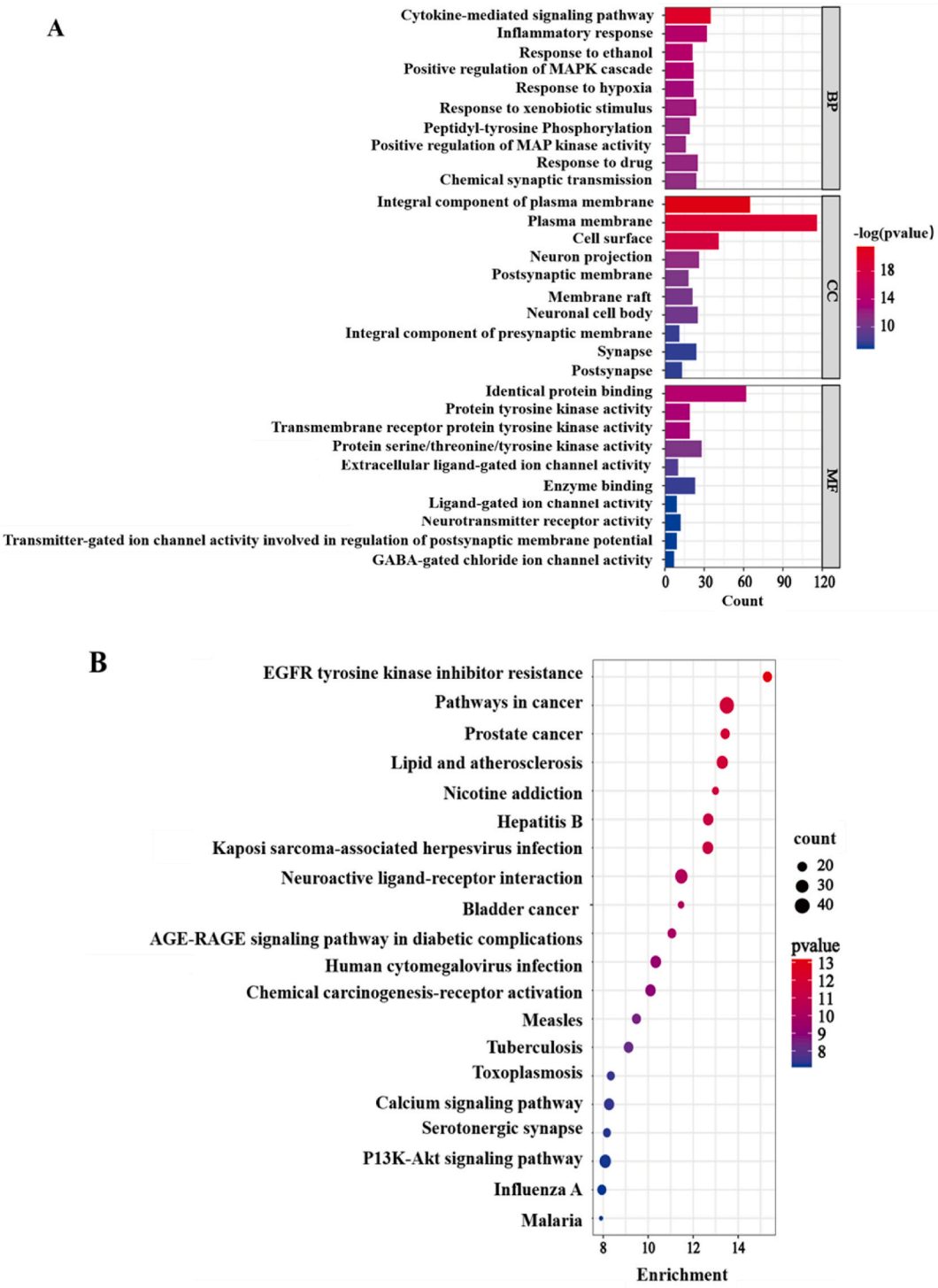

Fig. 3. The top 30 enriched GO terms (A) and top 20 enriched KEGG pathways (B) of ZP candidate targets. (The different color represents the significance of target gene enrichment.). (For interpretation of the references to color in this figure legend, the reader is referred to the Web version of this article.)

activity, and so on. CC terms were concentrated on the cytoplasm membrane and cell surface. MF terms mainly focused on identical protein binding and protein tyrosine kinase. The results of GO analysis showed that the active compounds in ZP could regulate protein binding and protein tyrosine kinase activity by affecting cellular component on the plasma membrane and cell surface, and might

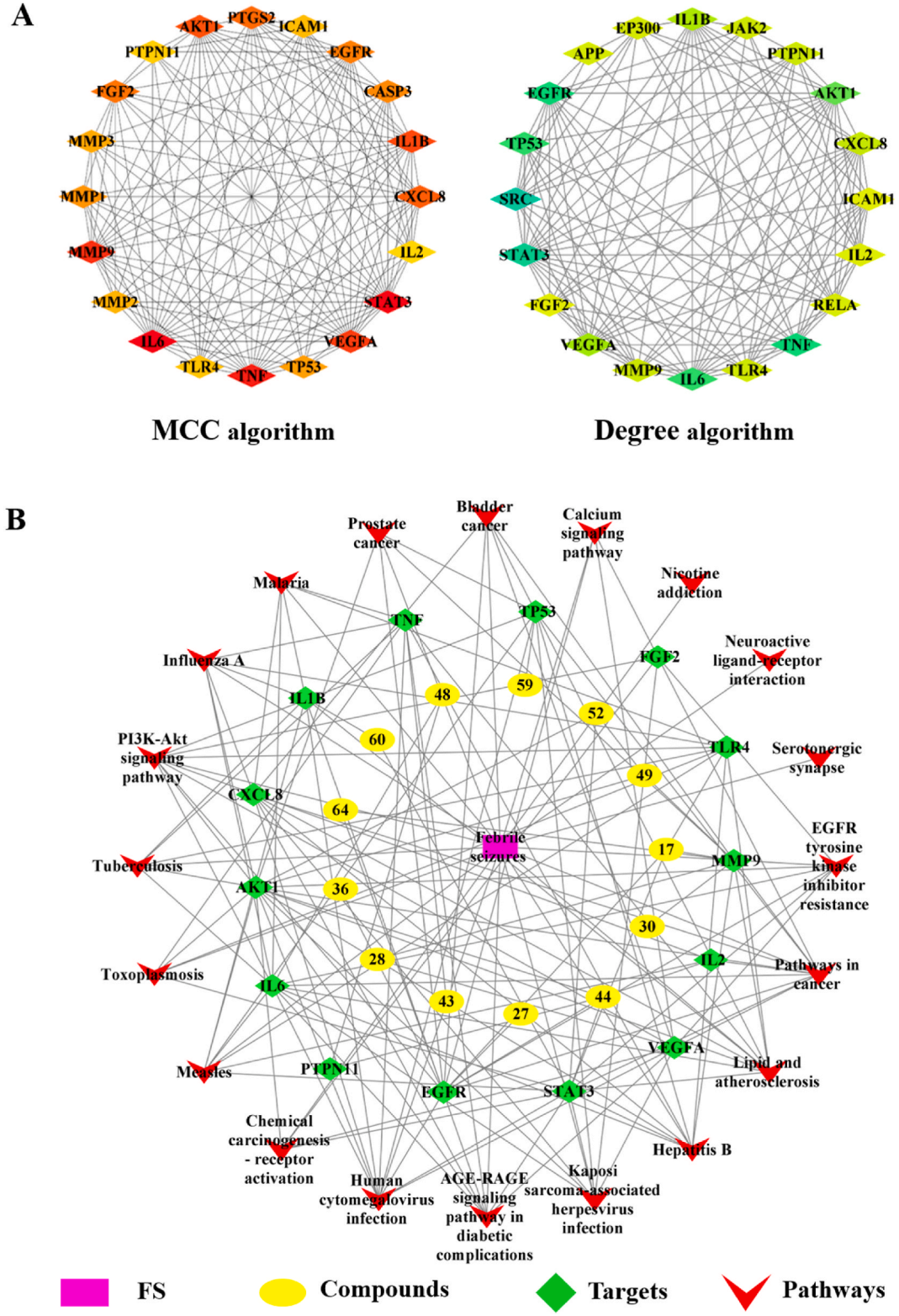

Fig. 4. The PPI network (A) and "compounds-targets-pathways-disease" network (B).

participate in signal pathways such as cytokines, inflammatory response, positive regulation of MAPK cascade pathway so as to exert antipyretic and anticonvulsant effects.

Furthermore, the top 20 enriched KEGG pathways were presented in Fig. 3B. The results showed that the EGFR tyrosine kinase inhibitor resistance was the main pathway, which is closely associated with excessive inflammatory response after central nervous system injury [37–39]. The inhibitors of EGFR signaling pathway can alleviate the inflammatory response and prevent the progression of inflammatory injury to improve the prognosis of secondary central nervous system injury, ultimately [40,41]. Additionally, the inflammatory response is involved in other pathways, including human cytomegalovirus infection, hepatitis B, and Kaposi sarcoma-associated herpesvirus infection. In view of this, it is hypothesized that ZP may play an anti-inflammatory role through EGFR tyrosine kinase inhibitor pathway to achieve treatment of FS.

3.4. The analysis of PPI network and construction of the "compounds-targets-pathways-disease" network

As the PPI network results displayed in Fig. 4A, the 14 genes that coexisted in two algorithms were regarded as core targets, including IL6, STAT3, TNF, MMP9, VEGFA, IL1B, AKT1, CXCL8, FGF2, EGFR, TP53, TLR4, PTPN11, and IL2. Among these genes, STAT3 is a functional protein involved in cell proliferation, differentiation, apoptosis, angiogenesis, inflammation, and immune response [42]. IL-6 is an important inflammatory cytokine, which can activate the STAT3 pathway, whereas IL-6/STAT3 is an essential pathway to mediate inflammatory signal transduction in cells [43,44]. In addition, EFGR, TNF, and other genes are associated with the regulation of inflammation, some of which are demonstrated closely relating to FS [45,46]. The levels of IL-6 in plasma and cerebrospinal fluid in patients with FS were higher than those in the control group [47]. It was also found that the injection of TNF-α into the hippocampus could reduce the time of seizures in the mouse epileptic model [48].

To further clarify the relationship between ZP and FS, a "compounds-targets-pathways-disease" network was constructed. Searching the targets of 21 components by the network discovered that only 13 components were closely associated with the 14 core targets, such as 6-hydroxy-2-(2-phenylethyl) chromone (compound 49), licochalcones B (compound 27), and 26-deoxycimicifugoside (compound 44). As shown in Fig. 4B, multiple components were connected to the focused targets, which were associated with the related pathways, indicating the characteristics of multi-ingredient, multi-target, and multi-pathway of TCM. It was reported that all the five derivatives of 2-(2-phenylethyl) chromone could effectively inhibit the production of nitric oxide by RAW264.7 cells due to lipopolysaccharide stimulation, which led to the inhibition of inflammation [49]. Moreover, the anti-inflammatory effects exerted by isoliquiritigenin and liquiritigenin in licorice [50]. Meanwhile, the results indicated that 14 targets such as IL6, STAT3, TNF, TLR4, VEGFA, and CXCL8 may play the important roles in the treatment of FS with ZP.

3.5. Molecular docking analysis

Molecular docking is a novel technology in the computer-aided molecular design field, which is widely applied to discover potential bioactive compounds and clarify the potential mechanisms between proteins and compounds [51,52]. To provide further evidence to support the identification of the potential active compounds, the binding of 13 compounds to 14 core targets was respectively verified by molecular docking. The original ligand was docked with the protein as the standard to evaluate the binding affinity and mode, respectively. According to the results shown in Fig. 5A and Table S4, most of the original ligands showed excellent binding activity with the target proteins and the scores ranging from −51.51 to −100.69 kcal/mol except for TNF (PDB ID: 2AZ5), IL1B (PDB ID: 5R88), and STAT3 (PDB ID: 5AX3), which showed moderate binding affinity. The results suggest that this mode was suitable for affinity prediction. Comparing with the original ligands, licochalcone B (compound 27) and licochalcone A (compound 64) showed good

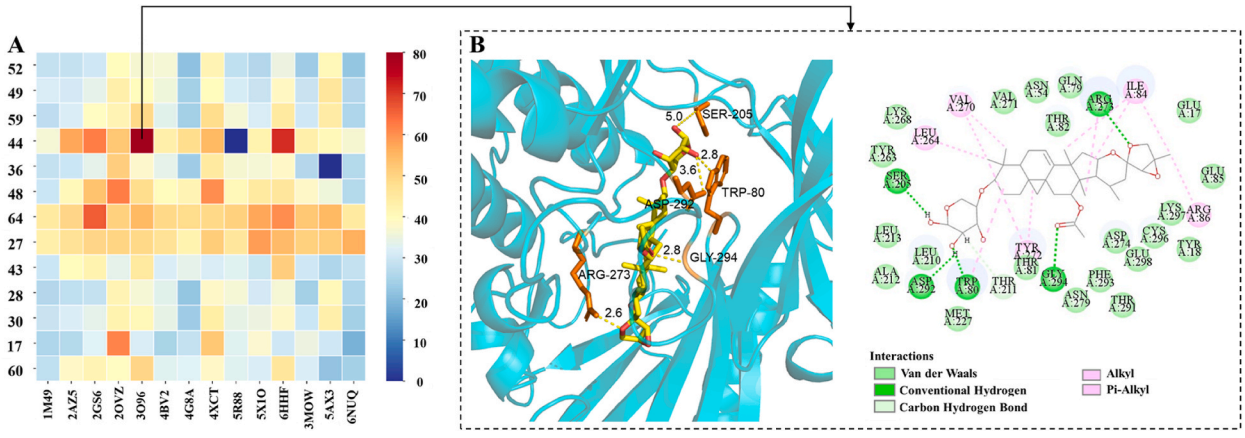

Fig. 5. Heat map of molecular docking results arranged in blue-red order by –CDocker interaction energy values (A) and binding map of 26-deoxycimicifugoside and 3O96 protein (B). (For interpretation of the references to color in this figure legend, the reader is referred to the Web version of this article.)

interactions with all target proteins (CDocker interaction energy ranging from −41.99 to −66.42 kcal/mol), which may demonstrate the multi-targeted interactions for treatment of FS. Additionally, 26-deoxycimicifugoside (compound 44) and hederagenin (compound 48) showed good binding with most of the target proteins. Notably, compound 44 bound to AKT1 (PDB ID: 3O96) with the score at −79.55 kcal/mol, which was superior to the original ligand with the score at −75.68 kcal/mol. While AKT1 (PDB ID: 3O96) exhibited the excellent binding interaction with most of the tested compounds, which was considered as the essential protein in anti-inflammation [53]. Meanwhile, compound 44 bound to EGFR (PDB ID: 2GS6) with the score at −62.32 kcal/mol, which was the key protein of the EGFR tyrosine kinase inhibitor pathway [54], showing the strong interaction comparing with the original ligand (score at −77.23 kcal/mol). Therefore, take compound 44 docked with AKT1 (PDB ID: 3O96) as an example. As shown in Fig. 5B, compound 44 bound to AKT1 (PDB ID: 3O96) mainly forming hydrogen bonds, which interacted with the protein at residues Arg-273$^{2.6}$, Gly-294$^{2.8}$, and Trp-80$^{2.8}$. The stability of the protein–ligand complex is predominantly determined by the hydrogen bonds, which are the major stabilizers for the complexes [55].

Licochalcones A and B have been demonstrated to have a wide range of biological effects, including antioxidant stress, anti-inflammatory, anticancer, antimicrobial, anti-Alzheimer's disease, and neuroprotective effects [56]. Hederagenin belongs to triterpenoid acid compounds, with various pharmacological effects such as anti-tumor, anti-depression, antibacterial, anti-inflammatory, and anti-diabetes [57]. Docking results indicate that ZP may have an important function in the treatment of FS by acting on 14 gene targets, primarily through the four compounds indicated above.

4. Conclusion

In this study, taking advantage of UPLC-Q-TOF-MS, 75 chemical components in ZP were characterized. Network pharmacology analysis explored 13 potential active ingredients and 14 key potential anti-FS targets relating to inflammatory response, EGFR tyrosine kinase inhibitor resistance, AGE-RAGE signaling pathway in diabetic complications, and neuroactive ligand-receptor interaction. Futhermore, licochalcones A and B, 26-deoxycimicifugoside, and hederagenin were screened as the main potential active ingredients by molecular docking. In summary, this study provides a reference for further research into the pharmacodynamic material basis and mechanism of ZP for the treatment of FS.

Data availability statement

Data will be made available on request.

CRediT authorship contribution statement

Lingling Song: Writing - review & editing, Writing - original draft, Visualization, Software, Investigation, Formal analysis, Data curation. **Jian Xu:** Writing - review & editing, Software, Formal analysis, Data curation. **Yanqiong Shi:** Writing - review & editing, Validation, Formal analysis. **Hemiao Zhao:** Writing - review & editing, Software, Formal analysis. **Min Zhang:** Writing - review & editing, Software, Formal analysis. **Yuefei Wang:** Writing - review & editing, Supervision, Project administration, Funding acquisition. **Ying Cui:** Writing - review & editing, Supervision, Project administration, Investigation. **Xin Chai:** Writing - review & editing, Supervision, Project administration, Investigation, Funding acquisition.

Declaration of competing interest

The authors declare that they have no known competing financial interests or personal relationships that could have appeared to influence the work reported in this paper.

Acknowledgements

This study was supported by the Science and Technology Project of Haihe Laboratory of Modern Chinese Medicine [No. 22HHZYSS00007 and 22HHZYJC00007], the Science and Technology Program of Tianjin [No. 22ZYJDSS00100], and the National Key Research and Development Program of China [No. 2021YFC1712905].

Appendix A. Supplementary data

Supplementary data to this article can be found online at https://doi.org/10.1016/j.heliyon.2023.e23865.

References

[1] L. Forsgren, R. Sidenvall, H.K. Blomquist, J. Heijbel, A prospective incidence study of febrile convulsions, Acta Paediatr. Scand. 79 (1990) 550–557, https://doi.org/10.1111/j.1651-2227.1990.tb11510.x.
[2] W.A. Hauser, The prevalence and incidence of convulsive disorders in children, Epilepsia 35 (1994), https://doi.org/10.1111/j.1528-1157.1994.tb05932.x.

[3] A.K. Leung, K.L. Hon, T.N. Leung, Febrile seizures: an overview, Drugs Context 7 (2018), 212536, https://doi.org/10.7573/dic.212536.
[4] M. Vestergaard, C.B. Pedersen, P. Sidenius, J. Olsen, J. Christensen, The long-term risk of epilepsy after febrile seizures in susceptible subgroups, Am. J. Epidemiol. 165 (2007) 911–918, https://doi.org/10.1093/aje/kwk086.
[5] J.W. Dreier, C.B. Pedersen, C. Cotsapas, J. Christensen, Childhood seizures and risk of psychiatric disorders in adolescence and early adulthood: a Danish nationwide cohort study, Lancet Child Adolesc. Health 2019 (2019) 99–108, https://doi.org/10.1016/S2352-4642(18)30351-1.
[6] A. Zare-shahabadi, S. Soltani, M.R. Ashrafi, A. Shahrokhi, S. Zoghi, B. Pourakbari, , et al.N. Rezaei, Association of IL4 single-nucleotide polymorphisms with febrile seizures, J. Child Neurol. 30 (2015) 423–428, https://doi.org/10.1177/0883073814551389.
[7] F. Tarhani, A. Nezami, G. Heidari, N. Dalvand, Factors associated with febrile seizures among children, Ann. Med. Surg (Lond). 75 (2022), 103360, https://doi.org/10.1016/j.amsu.2022.103360.
[8] M.R. Sharif, D. Kheirkhah, M. Madani, H.H. Kashani, The relationship between iron deficiency and febrile convulsion: a case-control study, Glob. J. Health Sci. 8 (2015) 185–189, https://doi.org/10.5539/gjhs.v8n2p185.
[9] A.H. Bakri, M.H. Hassan, A.E. Ahmed, P.R. Halim, S.A. El-Sawy, M.M. Mohamed, et al., Biochemical assessments of neurotrophin-3 and zinc involvement in the pathophysiology of pediatric febrile seizures: biochemical markers in febrile seizures, Biol. Trace Elem. Res. 200 (2022) 2614–2619, https://doi.org/10.1007/s12011-021-02886-w.
[10] Subcommittee on febrile seizures, American academy of pediatrics, Neurodiagnostic evaluation of the child with a simple febrile seizure, Pediatrics 127 (2011) 389–394, https://doi.org/10.1542/peds.2010-3318.
[11] H. Chen, S.C. Wang, Treatment of pediatric febrile seizure based on syndromes identification of “Heat, Phlegm, Fright and Wind”, J. Nanjing Univ. Tradit. Chin. Med. 37 (2021) 290–293, https://doi.org/10.14148/j.issn.1672-0482.2021.0290.
[12] E.J. Wang, A review on treating infant febrile convulsions in TCM medicine, Clin. J. Chin. Med. 6 (2014) 147–148, https://doi.org/10.3969/j.issn.1674-7860.2014.31.081.
[13] Chinese Pharmacopoeia Commission, Pharmacopoeia of People’s republic of China, China Medical Science Press, Beijing, 2020.
[14] J.Y. Wang, J.L. Liu, P. Liu, Comparison of pharmacological effects of Zixue Powder suspension in different ways of administration, Pharmacol. Clin. Chin. Mater. Med. (1998) 11–12.
[15] L. Li, J. Liu, J. Zhang, S.L. Ying, Therapeutic effect of Zixue Powder on collagen-induced arthritis in rats and its mechanism, Drug & Clin. 31 (2016) 1135–1140, https://doi.org/10.7501/j.issn.1674-5515.2016.08.003.
[16] Y.P. Zhang, Y.L. Lu, D. Sun, Z.M. Chen, Clinical observation on prevention of recurrent febrile seizure in children by short-term administration of Zixue, Inner Mongolia, J. Tradit. Chin. Med. 41 (2022) 1–3, https://doi.org/10.16040/j.cnki.cn15-1101.2022.05.007.
[17] J. Li, Y. Wang, R. Wang, M.Y. Wu, J. Shan, Y.C. Zhang, et al., Study on the molecular mechanisms of tetrandrine against pulmonary fibrosis based on network pharmacology, molecular docking and experimental verification, Heliyon 8 (2022), e10201, https://doi.org/10.1016/j.heliyon.2022.e10201.
[18] J.X. Li, Z.X. Han, X. Cheng, F.L. Zhang, J.Y. Zhang, Z.J. Su, et al., Combinational study with network pharmacology, molecular docking and preliminary experiments on exploring common mechanisms underlying the effects of weijing decoction on various pulmonary diseases, Heliyon 9 (2023), e15631, https://doi.org/10.1016/j.heliyon.2023.e15631.
[19] L. Pinzi, G. Rastelli, Molecular docking: shifting paradigms in drug discovery, Int. J. Mol. Sci. 20 (2019) 4331, https://doi.org/10.3390/ijms20184331.
[20] X. Jiao, X. Jin, Y. Ma, Y. Yang, J. Li, L. Liang, et al., A comprehensive application: molecular docking and network pharmacology for the prediction of bioactive constituents and elucidation of mechanisms of action in component-based Chinese medicine, Comput. Biol. Chem. 90 (2021), 107402, https://doi.org/10.1016/j.compbiolchem.2020.107402.
[21] W.I. Wu, W.C. Voegtli, H.L. Sturgis, F.P. Dizon, G.P. Vigers, B.J. Brandhuber, Crystal structure of human AKT1 with an allosteric inhibitor reveals a new mode of kinase inhibition, PLoS One 5 (2010), e12913, https://doi.org/10.1016/10.1371/journal.pone.0012913.
[22] J. Weisner, I. Landel, C. Reintjes, N. Uhlenbrock, M. Trajkovic-Arsic, N. Dienstbier, et al., Preclinical efficacy of covalent-allosteric AKT inhibitor borussertib in combination with trametinib in KRAS-mutant pancreatic and colorectal cancer, Cancer Res. 79 (2019) 2367–2378, https://doi.org/10.1158/0008-5472.
[23] X. Zhang, J. Gureasko, K. Shen, P.A. Cole, J. Kuriyan, An allosteric mechanism for activation of the kinase domain of epidermal growth factor receptor, Cell 125 (2006) 1137–1149, https://doi.org/10.1016/j.cell.2006.05.013.
[24] Y. Tsao, J. Liu, J. Kuo, W. Huang, W. Wu, Pi(4,5)P2 lipid binding induces a reorientation of FGF2 molecules near membrane surface to facilitate the unconventional oligomerization-dependent secretion process as revealed by a combined FTIR/NMR/X-Ray study, Biophys. J. 108 (2015), https://doi.org/10.1016/j.bpj.2014.11.1410, 255a-255a.
[25] C. Nichols, J. Ng, A. Keshu, G. Kelly, M.R. Conte, M.S. Marber, et al., Mining the PDB for tractable cases where X-ray crystallography combined with fragment screens can be used to systematically design protein-protein inhibitors: two test cases illustrated by IL1β-IL1R and p38α-TAB1 complexes, J. Med. Chem. 63 (2020) 7559–7568, https://doi.org/10.1021/acs.jmedchem.
[26] M.R. Arkin, M. Randal, W.L. DeLano, J. Hyde, T.N. Luong, J.D. Oslob, et al., Binding of small molecules to an adaptive protein-protein interface, Proc. Natl. Acad. Sci. USA 100 (2003) 1603–1608, https://doi.org/10.1073/pnas.252756299.
[27] A. Tochowicz, K. Maskos, R. Huber, R. Oltenfreiter, V. Dive, A. Yiotakis, et al., Crystal structures of MMP-9 complexes with five inhibitors: contribution of the flexible Arg424 side-chain to selectivity, J. Mol. Biol. 371 (2007) 989–1006, https://doi.org/10.1016/j.jmb.2007.05.068.
[28] E. Nuti, A.R. Cantelmo, C. Gallo, A. Bruno, B. Bassani, C. Camodeca, et al., N-O-isopropyl sulfonamido-based hydroxamates as matrix metalloproteinase inhibitors: hit selection and in vivo antiangiogenic activity, J. Med. Chem. 58 (2015) 7224–7240, https://doi.org/10.1021/acs.jmedchem.5b00367.
[29] Zhang Z.Y., Liu S., Yu Z., Yu X. Crystal structure of SHP2 in complex with a tautomycetin analog TTN D-1, doi: 10.2210/pdb3mow/pdb.
[30] T. Kinoshita, H. Sugiyama, Y. Mori, N. Takahashi, A. Tomonaga, Identification of allosteric ERK2 inhibitors through in silico biased screening and competitive binding assay, Bioorg. Med. Chem. Lett. 26 (2016) 955–958, https://doi.org/10.1016/j.bmcl.2015.12.056.
[31] L. Bai, H. Zhou, R. Xu, Y. Zhao, K. Chinnaswamy, D. McEachern, et al., A potent and selective small-molecule degrader of STAT3 achieves complete tumor regression in vivo, Cancer Cell 36 (2019) 498–511, https://doi.org/10.1016/j.ccell.2019.10.002.
[32] U. Ohto, N. Yamakawa, S. Akashi-Takamura, K. Miyake, T. Shimizu, Structural analyses of human Toll-like receptor 4 polymorphisms D299G and T399I, J. Biol. Chem. 287 (2012) 40611–40617, https://doi.org/10.1074/jbc.M112.404608.
[33] M.M. He, A.S. Smith, J.D. Oslob, W.M. Flanagan, A.C. Braisted, A. Whitty, et al., Small-molecule inhibition of TNF-alpha, Science 310 (2005) 1022–1025, https://doi.org/10.1126/science.1116304.
[34] M. Gertz, F. Fischer, G.T. Nguyen, M. Lakshminarasimhan, M. Schutkowski, M. Weyand, Ex-527 inhibits sirtuins by exploiting their unique nad+-dependent deacetylation mechanism, Proc. Natl. Acad. Sci. USA 110 (2013) E2772–E2781, https://doi.org/10.1073/pnas.1303628110.
[35] C.Y. Yi, Study on the treatment of infantile febrile convulsion with integrated Chinese and Western medicine, J. Med. Theor. & Prac. 27 (2014) 3039–3040, https://doi.org/10.19381/j.issn.1001-7585.2014.22.062.
[36] H.Y. Zhang, J. Hu, X. Han, L. Zhang, X.J. Zhu, W. Song, et al., Anticonvulsant effect of different processes of Zixue Powder in mice and its mechanism, Drug Eval. Res. 45 (2022) 84–89, https://doi.org/10.7501/j.issn.1674-6376.2022.01.010.
[37] D.A. Sabbah, R. Hajjo, K. Sweidan, Review on epidermal growth factor receptor (EGFR) structure, signaling pathways, interactions, and recent updates of EGFR inhibitors, Curr. Top Med. Chem. 20 (2020) 815–834, https://doi.org/10.2174/1568026620666200303123102.
[38] Z.W. Li, J.J. Zhao, S.Y. Li, T.T. Cao, Y. Wang, Y. Guo, et al., Blocking the EGFR/p38/NF-κB signaling pathway alleviates disruption of BSCB and subsequent inflammation after spinal cord injury, Neurochem. Int. 150 (2021), 105190, https://doi.org/10.1016/j.neuint.2021.105190.
[39] X.J. Cai, Z. Jiao, B.Y. Ren, Y. Lu, X.H. Zhang, H. Wen, et al., Epidermal growth factor receptor signaling pathway activation mediating inflammatory damage in central nervous system, Chin. J. Neuromed. 17 (2018) 199–204, https://doi.org/10.1007/s12035-010-8115-7.
[40] M. Wu, P. Zhang, EGFR-mediated autophagy in tumourigenesis and therapeutic resistance, Cancer Lett. 469 (2020) 207–216, https://doi.org/10.1016/j.canlet.2019.10.030.
[41] Z.W. Li, D.M. Jiang, J. Han, J.M. Tu, Q. Wang, Protective effect of EGFR inhibitor on blood spinal barrier damage induced by oxygen glucose deprivation/re-oxygenation, Neural Injury and Functional Reconstruction 16 (2021) 63–66+89, https://doi.org/10.16780/j.cnki.sjssgncj.20201240.

[42] A. Subramaniam, M.K. Shanmugam, E. Perumal, F. Li, A. Nachiyappan, X. Dai, et al., Potential role of signal transducer and activator of transcription (STAT)3 signaling pathway in inflammation, survival, proliferation and invasion of hepatocellular carcinoma, Biochim. Biophys. Acta 1835 (2013) 46–60, https://doi.org/10.1016/j.bbcan.2012.10.002.
[43] H. Yu, D. Pardoll, R. Jove, STATs in cancer inflammation and immunity: a leading role for STAT3, Nat. Rev. Cancer 9 (2009) 798–809, https://doi.org/10.1038/nrc2734.
[44] T. Hirano, IL-6 in inflammation, autoimmunity and cancer, Int. Immunol. 33 (2021) 127–148, https://doi.org/10.1093/intimm/dxaa078.
[45] J. Choi, H.J. Min, J.S. Shin, Increased levels of HMGB1 and pro-inflammatory cytokines in children with febrile seizures, J. Neuroinflammation 8 (2011) 135, https://doi.org/10.1186/1742-2094-8-135.
[46] X. Li, S. Guo, K. Liu, C. Zhang, H. Chang, W. Yang, et al., GABRG2 deletion linked to genetic epilepsy with febrile seizures plus affects the expression of $GABA_A$ receptor subunits and other genes at different temperatures, Neuroscience 438 (2020) 116–136, https://doi.org/10.1016/j.neuroscience.2020.04.049.
[47] M. Virta, M. Hurme, M. Helminen, Increased plasma levels of pro- and anti-inflammatory cytokines in patients with febrile seizures, Epilepsia 43 (2002) 920–923, https://doi.org/10.1046/j.1528-1157.2002.02002.x.
[48] S. Balosso, T. Ravizza, C. Perego, J. Peschon, I.L. Campbell, et al., Tumor necrosis factor-alpha inhibits seizures in mice via p75 receptors, Ann. Neurol. 57 (2005) 804–812, https://doi.org/10.1002/ana.20480.
[49] H.X. Huo, Y.F. Gu, H. Sun, Y.F. Zhang, W.J. Liu, Z.X. Zhu, et al., Anti-inflammatory 2-(2-phenylethyl)chromone derivatives from Chinese agarwood, Fitoterapia 118 (2017) 49–55, https://doi.org/10.1016/j.fitote.2017.02.009.
[50] V. Babu, D.S. Kapkoti, M. Binwal, R.S. Bhakuni, K. Shanker, M. Singh, et al., Liquiritigenin, isoliquiritigenin rich extract of *Glycyrrhiza glabra* roots attenuates inflammation in macrophages and collagen-induced arthritis in rats, Inflammopharmacology 31 (2023) 983–996, https://doi.org/10.1007/s10787-023-01152-w.
[51] K. Attala, M.S. Eissa, M.M. El-Henawee, S.S.A. El-Hay, Application of quality by design approach for HPTLC simultaneous determination of amlodipine and celecoxib in presence of process-related impurity, Microchem. J. 162 (2020), 105857, https://doi.org/10.1016/j.microc.2020.105857.
[52] K. Attala, A. Elsonbaty, A.E. Mostafa, M.S. Eissa, G.M. Hadad, M.A. Abdelshakour, et al., In-Silico analytical chemistry contributions to analytical and bio-analytical applications in spectroscopic and chromatographic techniques: molecular, mechanical and quantum insights, Rec. Pharm. Biomed. Sci. 7 (2023) 125–144, https://doi.org/10.21608/rpbs.2023.190923.1211.
[53] C. Zhao, X. Yang, E.M. Su, Y. Huang, L. Li, M.A. Matthay, et al., Signals of vagal circuits engaging with AKT1 in α7 nAChR+CD11b+ cells lessen E. coli and LPS-induced acute inflammatory injury, Cell Discov. 3 (2017), 17009, https://doi.org/10.1038/celldisc.2017.9.
[54] K. Kobayashi, A.C. Tan, Unraveling the impact of intratumoral heterogeneity on EGFR tyrosine kinase inhibitor resistance in EGFR-mutated NSCLC, Int. J. Mol. Sci. 24 (2023) 4126, https://doi.org/10.3390/ijms24044126.
[55] A. Zhou, X. Li, J. Zou, L. Wu, B. Cheng, J. Wang, Discovery of potential quality markers of *Fritillariae thunbergii* bulbus in pneumonia by combining UPLC-QTOF-MS, network pharmacology, and molecular docking, Mol. Divers. 26 (2023) 1–18, https://doi.org/10.1007/s11030-023-10620-y.
[56] G.D. Maria Pia, F. Sara, F. Mario, S. Lorenza, Biological effects of licochalcones, Mini Rev. Med. Chem. 19 (2019) 647–656, https://doi.org/10.2174/1389557518666180601095420.
[57] J. Zeng, T. Huang, M. Xue, J. Chen, L. Feng, R. Du, et al., Current knowledge and development of hederagenin as a promising medicinal agent: a comprehensive review, RSC Adv. 8 (2018) 24188–24202, https://doi.org/10.1039/c8ra03666g.